Inorganic Chemistry

Article

Incorporation of Substitutionally Labile [V^{III}(CN)$_6$]$^{3-}$ into Prussian Blue Type Magnetic Materials

Kendric J. Nelson and Joel S. Miller*

Department of Chemistry, University of Utah, 315 South 1400 East, Room 2020, Salt Lake City, Utah 84112-0850

A Prussian blue (PB) type material containing hexacyanovanadate(III), Mn$^{II}_{1.5}$[V^{III}(CN)$_6$]$\cdot$0.30MeCN (**1**), was formed from the reaction of [V^{III}(CN)$_6$]$^{3-}$ with [Mn(NCMe)$_6$]$^{2+}$ in MeCN. This new material exhibits ferrimagnetic spin- or cluster-glass behavior below a T_c of 12 K with observed magnetic hysteresis at 2 K ($H_{cr} = 65$ Oe and $M_{rem} = 730$ emu$\cdot$Oe/mol). Reactions of [V^{III}(CN)$_6$]$^{3-}$ with [M^{II}(NCMe)$_6$]$^{2+}$ (M = Fe, Co, Ni) in MeCN lead to either partial (M = Co) or complete (M = Fe, Ni) linkage isomerization, resulting in compounds of Fe$^{II}_{0.5}$V^{III}[Fe^{II}(CN)$_6$]$\cdot$0.85MeCN (**2**), (NEt$_4$)$_{0.10}$Co$^{II}_{1.5-a}$V$^{II}_a$[Co^{III}(CN)$_6$]$_a$[V^{III}(CN)$_6$]$_{1-a}$(BF$_4$)$_{0.10}\cdot$0.35MeCN (**3**), and (NEt$_4$)$_{0.20}$V^{III}[Ni^{II}(CN)$_4$]$_{1.6}\cdot$0.10MeCN (**4**) compositions. Compounds **2–4** do not magnetically order as a consequence of diamagnetic cyanometalate anions being present, i.e., [Fe^{II}(CN)$_6$]$^{4-}$, [Co^{III}(CN)$_6$]$^{3-}$, and [Ni^{II}(CN)$_4$]$^{2-}$. Incorporation of [V^{III}(CN)$_6$]$^{3-}$ into PB-type materials is synthetically challenging because of the lability of the cyanovanadate(III) anion.

Introduction

The synthesis of Prussian blue (PB) and its analogues, leading to new molecule-based magnetic materials, has been a contemporary research focus.[1] Molecule-based magnets have potential uses in many areas including magnetic shielding[2] and spintronic memory storage devices.[3] Prussian blue analogues (PBAs) are generally synthesized by mixing a substitutionally labile [M(Solvent)$_x$]$^{n+}$ cation with a substitutionally inert [M′(CN)$_6$]$^{m-}$ anion in aqueous media to form A$_a$M$_b$[M′(CN)$_6$]$_c\cdot z$Solvent, which adopts a face-centered-cubic (fcc) structure with unit cell length $a = 10.4 \pm 0.5$ Å.[4,5] Because of the electronic and spin-state differences available to both M^{II} and M′, PBAs can be tailored to possess numerous metal ions that vary in the charge and number of spins per metal site and thus can lead to a variety of magnetic behaviors.[1]

Incorporating the cyanovanadate(III) anion into PB materials has proven challenging because it is hydrolytically unstable in aqueous media.[6] However, with the advent of the nonaqueous soluble cyanovanadate(III) anion in (NEt$_4$)$_3$[V^{III}(CN)$_6$][7], it was anticipated that incorporation of [V^{III}(CN)$_6$]$^{3-}$ into PB materials by nonaqueous routes was possible. Initial attempts to synthesize PB materials possessing hexacyanovanadate(III) were unsuccessful, because while

* To whom correspondence should be addressed. E-mail: jsmiller@chem.utah.edu.

(1) (a) Mallah, T.; Thiébaut, S.; Verdaguer, M.; Veillet, P. *Science* **1993**, *262*, 1554. (b) Ferlay, S.; Mallah, T.; Ouahes, R.; Veillet, P.; Verdaguer, M. *Nature* **1995**, *378*, 701. (c) Buschmann, W. E.; Paulson, S. C.; Wynn, C. M.; Girtu, M.; Epstein, A. J.; White, H. S.; Miller, J. S. *Adv. Mater.* **1997**, *9*, 645. (d) Buschmann, W. E.; Paulson, S. C.; Wynn, C. M.; Girtu, M.; Epstein, A. J.; White, H. S.; Miller, J. S. *Chem. Mater.* **1998**, *10*, 1386. (e) Dujardin, E.; Ferlay, S.; Phan, X.; Desplanches, C.; Moulin, C. C. D.; Sainctavit, P.; Baudelet, F.; Dartyge, E.; Veillet, P.; Verdaguer, M. *J. Am. Chem. Soc.* **1998**, *120*, 11347. (f) Ferlay, S.; Mallah, T.; Ouahes, R.; Veillet, P.; Verdaguer, M. *Inorg. Chem.* **1999**, *38*, 229. (g) Verdaguer, M.; Bleuzen, A.; Marvaud, V.; Vaissermann, J.; Seuleiman, M.; Desplanches, C.; Scuiller, A.; Train, C.; Garde, R.; Gelly, G.; Lomenech, C.; Rosenman, I.; Veillet, P.; Cartier, C.; Villain, F. *Coord. Chem. Rev.* **1999**, *190–192*, 1023. (h) Verdaguer, M.; Bleuzen, A.; Train, C.; Garde, R.; Fabrizi de Biani, F.; Desplanches, C. *Philos. Trans. R. Soc. London, Ser. A* **1999**, *357*, 2959. (i) Hashimoto, K.; Ohkoshi, S. *Philos. Trans. R. Soc. London, Ser. A* **1999**, *357*, 2977. (j) HatlevikØ.; Buschmann, W. E.; Zhang, J.; Manson, J. L.; Miller, J. S. *Adv. Mater.* **1999**, *11*, 914. (k) Holmes, S. M.; Girolami, G. S. *J. Am. Chem. Soc.* **1999**, *121*, 5593. (l) Verdaguer, M.; Girolami, G. S. In *Magnetism—Molecules to Materials*; Miller, J. S., Drillon, M., Eds.; Wiley-VCH: Weinheim, Germany, 2005; Vol. 5, pp 283–346.

(2) (a) Landee, C. P.; Melville, D.; Miller, J. S. In *NATO ARW Molecular Magnetic Materials*; Kahn, O., Gatteschi, D., Miller, J. S., Palacio, F., Eds.; Kluwer Academic Publishers: London, 1991; Vol. *E198*, p 395. (b) Morin, B. G.; Hahm, C.; Epstein, A. J.; Miller, J. S. *J. Appl. Phys.* **1994**, *75*, 5782. (c) Miller, J. S. *Adv. Mater.* **1994**, *6*, 322.

(3) Prigodin, V. N.; Raju, N. P.; Pokhodnya, K. I.; Miller, J. S.; Epstein, A. J. *Adv. Mater.* **2002**, *14*, 1230.

(4) Verdaguer, M.; Girolami, G. S. In *Magnetism—Molecules to Materials*; Miller, J. S., Drillon, M., Eds.; Wiley-VCH: Weinheim, Germany, 2005; Vol. 5, pp 283–346.

(5) (a) Ludi, A.; Güdel, H. U. *Struct. Bonding (Berlin)* **1973**, *14*, 1. (b) Dunbar, K. R.; Heintz, R. A. *Prog. Inorg. Chem.* **1997**, *45*, 283.

(6) Levenson, R. A.; Dominguez, R. J. G.; Willis, M. A.; Young, F. R., III. *Inorg. Chem.* **1974**, *13*, 2761.

the reaction of (NEt$_4$)$_3$[V^{III}(CN)$_6$] with [Cr^{II}(NCMe)$_4$](BF$_4$)$_2$ in MeCN formed Cr$_{1.5}$[V(CN)$_6$]·zMeCN, electron transfer between Cr^{II} and V^{III} occurs and the product is best formulated as Cr$^{II}_{0.5}$Cr^{III}[V^{II}(CN)$_6$]·zMeCN.[7] An exception was the formation of Cr^{III}[V^{III}(CN)$_6$] using the unconventional [Cr^{III}(NCMe)$_6$]$^{3+}$ nonaqueous labile source of Cr^{III} and [V^{III}(CN)$_6$]$^{3-}$.[8] With the goal to prepare [V^{III}(CN)$_6$]$^{3-}$-based PB-type magnets, the reaction of [V^{III}(CN)$_6$]$^{3-}$ with [M^{II}-(NCMe)$_6$]$^{2+}$ was investigated in nonaqueous media, and herein we report the reactions involving M^{II} (M = Mn, Fe, Co, Ni) and the formation of a new [V^{III}(CN)$_6$]$^{3-}$-based magnet.

Experimental Section

All manipulations were carried out under a dry N$_2$ atmosphere (<1 ppm O$_2$) using Schlenck techniques or in a Vacuum Atmospheres DriLab. [Mn^{II}(NCMe)$_6$](SbF$_6$)$_2$,[9] [M^{II}(NCMe)$_6$](BF$_4$)$_2$ (M = Fe, Co, Ni),[10] and (NEt$_4$)$_3$[V^{III}(CN)$_6$][7] were prepared via literature routes. Acetonitrile (MeCN) was purified through an activated alumina dual-column purification system under a positive pressure of N$_2$, while tetrahydrofuran (THF) was purified via distillation under positive dry N$_2$ pressure using sodium dispersion (Strem) and benzophenone (Lancaster).

Physical Methods. IR spectra were recorded from 400 to 4000 cm^{-1} on a Bruker Tensor 37 IR spectrophotometer (±1 cm^{-1}) as KBr pellets. Centrifugation of samples was performed using a Clay Adams centrifuge with a fixed rotary speed of 3200 rpm. Samples were centrifuged for 10 min to separate the solid precipitates from the mother liquor. Thermogravimetric analyses coupled with mass spectroscopy (TGA/MS) measurements were performed on a TA Instruments model 2050 TGA analyzer coupled to a Thermolab TL1285 thermal analysis mass spectrometer. The TGA operates between ambient temperature and 1000 °C and is located in a Vacuum Atmospheres DriLab under an inert atmosphere. TGA samples were handled in a N$_2$ atmosphere and heated under a N$_2$ purge. Heating rates were 10 °C/min. Elemental analyses were performed by GCL & Chemisar Laboratories (Guelph, Ontario, Canada) on freshly prepared samples that were sealed under a dry N$_2$ atmosphere.

Powder X-ray diffraction (PXRD) scans were obtained on a $\theta\angle\theta$ Bruker AXS D8 Advance diffractometer (2θ of 12.5–42.5°, step width of 0.02°, counting time of 10 s/step, voltage of 40 kV, and current of 40 mA) fitted with a Göbel mirror to remove all but the Cu Kα radiation (γ = 1.540 60 Å). Samples were sealed under an inert atmosphere in 1.00 mm thin-walled quartz capillaries to prevent oxidation/moisture absorption, and scans were performed at room temperature (~298 K).

Magnetic susceptibility measurements were made between 2 and 300 K using a Quantum Design MPMS-5 5T SQUID magnetometer with a sensitivity of 10^{-8} emu or 10^{-12} emu/Oe at 1 T and equipped with the ultralow-field (~0.005 Oe), reciprocating sample measurement system, and continuous low-temperature control with enhanced thermometry features, or using a Quantum Design PPMS-9 susceptometer. Measurements were made on powders contained in airtight Delrin holders supplied by Quantum Design. Small amounts

of quartz wool were used in the Delrin holders to minimize the movement of the powders during measurements. The data were corrected for the measured diamagnetism of each holder, and core diamagnetic corrections of −117, −131, −131, and −133 × 10^{-6} emu/mol were calculated from Pascal's constants for Mn$_{1.5}$[V(CN)$_6$]·0.30MeCN (**1**), Fe$_{0.5}$V[Fe(CN)$_6$]·0.85MeCN (**2**), (NEt$_4$)$_{0.10}$Co$_{1.5-a}$V$_a$[Co(CN)$_6$]$_a$[V(CN)$_6$]$_{1-a}$(BF$_4$)$_{0.10}$·0.35MeCN (**3**),[11] and (NEt$_4$)$_{0.20}$V[Ni(CN)$_4$]$_{1.6}$·0.10MeCN (**4**).

Mn$^{II}_{1.5}$[V^{III}(CN)$_6$]·0.30MeCN (1). 1 was synthesized by slowly adding a 10 mL MeCN solution of (NEt$_4$)$_3$[V^{III}(CN)$_6$] (114.1 mg, 0.191 mmol, 1.0 equiv) via a syringe pump at 1 mL/h into a stirring 20 mL MeCN solution of [Mn^{II}(NCMe)$_6$](SbF$_6$)$_2$ (221.6 mg, 0.2868 mmol, 1.5 equiv). This forms an immediate dark-brown precipitate. After complete addition of the V^{III} solution, the mixture was stirred for approximately 12 h. The dark-brown product was collected via centrifugation, and the colorless supernate was decanted. The product was washed with MeCN (3 × 10 mL), followed by 10 mL of THF, and dried at room temperature under vacuum for 12 h. A dark-brown solid was isolated in a quantitative yield. Anal. Calcd for Mn$^{II}_{1.5}$[V^{III}(CN)$_6$]·0.30MeCN, C$_{6.60}$H$_{0.90}$N$_{6.30}$Mn$_{1.50}$V$_{1.00}$: C, 26.27; H, 0.30; N, 29.24; Mn, 27.31; V, 16.88. Found: C, 26.66; H, 0.83; N, 28.35; Mn, 27.35; V, 14.77.[12] TGA/MS analysis (vide infra) showed that the sample was thermally unstable at relatively low temperatures (50 °C), above which solvent loss and decomposition occur simultaneously. IR (KBr): ν_{CN} = 2130 (s) [half-width at half-height (hwhh): 43 cm^{-1}] as well as 2282 (w) and 2311 (w) cm^{-1} (MeCN).

Fe$^{II}_{0.5}$V^{III}[Fe^{II}(CN)$_6$]·0.85MeCN (2). 2 was synthesized by slowly adding a 10 mL MeCN solution of (NEt$_4$)$_3$[V^{III}(CN)$_6$] (116.7 mg, 0.1952 mmol, 1.0 equiv) via a syringe pump at 1 mL/h into a stirring 20 mL MeCN solution of [Fe^{II}(NCMe)$_6$](BF$_4$)$_2$ (139.2 mg, 0.293 mmol, 1.5 equiv). This forms an immediate dark-brown precipitate. After complete addition of the V^{III} solution, the mixture was stirred for approximately 12 h. The dark-brown product was collected via centrifugation, and the colorless supernate was decanted. The product was washed with MeCN (3 × 10 mL), followed by 10 mL of THF, and dried at room temperature under vacuum for 12 h. A dark-brown solid was isolated in a quantitative yield. Anal. Calcd for Fe$^{II}_{0.5}$V^{III}[Fe^{II}(CN)$_6$]·0.85MeCN, C$_{7.70}$H$_{2.55}$N$_{6.85}$Fe$_{1.50}$V$_{1.00}$: C, 28.39; H, 0.79; N, 29.46; Fe, 25.72; V, 15.64. Found: C, 28.00; H, 1.52; N, 29.83; Fe, 25.30; V, 16.07. TGA/MS analysis (vide infra) showed that the sample was thermally unstable at relatively low temperatures (50 °C), above which solvent loss and decomposition occur simultaneously. IR (KBr): ν_{CN} = 2081 (s) (hwhh: 50 cm^{-1}) as well as 2287 (vw) and 2313 (vw) cm^{-1} (MeCN).

(NEt$_4$)$_{0.10}$Co$^{II}_{1.5-a}$V$^{II}_a$[Co^{III}(CN)$_6$]$_a$[V^{III}(CN)$_6$]$_{1-a}$(BF$_4$)$_{0.10}$·0.35-MeCN (3). 3 was synthesized by slowly adding a 10 mL MeCN solution of (NEt$_4$)$_3$[V^{III}(CN)$_6$] (126.0 mg, 0.211 mmol, 1.0 equiv) via a syringe pump at 1 mL/h into a stirring 20 mL MeCN solution of [Co^{II}(NCMe)$_6$](BF$_4$)$_2$ (152.3 mg, 0.318 mmol, 1.5 equiv). This forms an immediate dark-blue precipitate. After complete addition of the V^{III} solution, the mixture was stirred for approximately 12 h. The dark-blue product was collected via centrifugation, and the colorless supernate was decanted. The product was washed with MeCN (3 × 10 mL), followed by 10 mL of THF, and dried at room temperature under vacuum for 12 h. A dark-blue solid was isolated in a quantitative yield. Anal. Calcd for (NEt$_4$)$_{0.10}$-

(7) Nelson, K. J.; Giles, I. D.; Troff, S. A.; Arif, A. M.; Miller, J. S. *Inorg. Chem.* **2006**, *45*, 8922.

(8) Nelson, K. J.; Daniels, M. C.; Reiff, W. M.; Troff, S. A.; Miller, J. S. *Inorg. Chem.* **2007**, *46*, 10093.

(9) Vickers, E. B.; Giles, I. D.; Miller, J. S. *Chem. Mater.* **2005**, *17*, 1667.

(10) Heintz, R. A.; Smith, J. A.; Szalay, P. S.; Weisgerber, A.; Dunbar, K. R.; Beck, K.; Coucouvanis, D. *Inorg. Synth.* **2002**, *33*, 75.

(11) The formula (NEt$_4$)$_{0.10}$Co$_{1.5-a}$V$_a$[Co(CN)$_6$]$_a$[V(CN)$_6$]$_{1-a}$(BF$_4$)$_{0.10}$·0.35-MeCN shows that the cyanide is C-bound to both the V and Co ions, which was confirmed by IR analysis.

(12) The percent of V had a larger than desired deviation in samples **1** and **4** and is attributed to inaccurate measurements. In both cases, all four other elements fit reasonably well.

Table 1. Characteristic IR ν_{CN} Absorptions as Well as the Colors of **1–4**

	color	ν_{CN} (cm^{-1}) (hwhh, cm^{-1})	ν_{CN} (cm^{-1}), $(NEt_4)_3[V^{III}(CN)_6]$	$\Delta\nu_{CN}$ (cm^{-1})^a
1	dark brown	2130 (43)	2107	23
2	dark brown	2081 (50)	2107	−26
3	dark blue	2121 (30), 2161 (25)	2107	14, 54
4	dark violet	2168 (28)	2107	61

^{a} $\Delta\nu_{CN}$ is the shift in ν_{CN} with respect to the parent cyanometalate complex upon bridging of the V to the second metal.

$Co^{II}_{1.5-a}V^{II}_a[Co^{III}(CN)_6]_a[V^{III}(CN)_6]_{1-a}(BF_4)_{0.10} \cdot 0.35MeCN$, $C_{7.50}H_{3.05}N_{6.45}Co_{1.50}V_{1.00}$: C, 27.17; H, 0.93; N, 27.25; Co, 26.66; V, 15.37. Found: C, 27.49; H, 0.74; N, 27.36; Co, 27.06; V, 14.85. TGA/MS analysis (vide infra) showed that the sample was thermally unstable at relatively low temperatures (50 °C), above which solvent loss and decomposition occur simultaneously. IR (KBr): ν_{CN} = 2121(s) and 2161 (s) (hwhh: 30 and 25 cm^{-1}) as well as 2287 (vw) and 2313 (vw) cm^{-1} (MeCN).

$(NEt_4)_{0.20}V^{III}[Ni^{II}(CN)_4]_{1.6} \cdot 0.10MeCN$ (4). 4 was synthesized by slowly adding a 10 mL MeCN solution of $(NEt_4)_3[V^{III}(CN)_6]$ (119.7 mg, 0.200 mmol, 1.0 equiv) via a syringe pump at 1 mL/h into a stirring 20 mL MeCN solution of $[Ni^{II}(NCMe)_6](BF_4)_2$ (144.4 mg, 0.302 mmol, 1.5 equiv). This forms an immediate dark-violet precipitate. After complete addition of the V^{III} solution, the mixture was stirred for approximately 12 h. The dark-violet product was collected via centrifugation, and the colorless supernate was decanted. The product was washed with MeCN (3 × 10 mL), followed by 10 mL of THF, and dried at room temperature under vacuum for 12 h. A dark-violet solid was isolated in a quantitative yield. Anal. Calcd for $(NEt_4)_{0.20}V^{III}[Ni^{II}(CN)_4]_{1.6} \cdot 0.10MeCN$, $C_{8.20}H_{4.30}N_{6.70}Ni_{1.60}V_{1.00}$: C, 28.84; H, 1.27; N, 27.48; Ni, 27.50; V, 14.91. Found: C, 28.67; H, 0.93; N, 27.52; Ni, 27.77; V, 13.45.[12] TGA/MS analysis (vide infra) showed that the sample was thermally unstable at relatively low temperatures (50 °C), above which solvent loss and decomposition occur simultaneously. IR (KBr): ν_{CN} = 2168 (s) (hwhh: 28 cm^{-1}) as well as 2289 (vw) and 2314 (vw) cm^{-1} (MeCN).

Results and Discussion

Synthesis. The slow addition of $(NEt_4)_3[V^{III}(CN)_6]$ to $[M^{II}(NCMe)_6]^{2+}$ [M = Mn, Fe, Co, Ni] in MeCN solutions led to the formation of four dark-colored precipitates of **1**, **2**, **3**,[11] and **4** compositions (Table 1). All of these deeply colored solids are very air- and moisture-sensitive and were therefore handled under a dry N_2 atmosphere.[13] The compositions of these materials were determined by elemental analysis,[14] and the assignments of oxidation states were made from stoichiometry as well as the analysis of the ν_{CN} IR absorptions.

IR Spectra. The ν_{CN} absorptions for compounds **1–4** are displayed in Figure S1 in the Supporting Information and summarized in Table 1. Compound **1** exhibits a broad ν_{CN} absorption at 2130 cm^{-1} (hwhh: 43 cm^{-1}), which is shifted to higher frequency with respect to the $[V^{III}(CN)_6]^{3-}$ parent

cyanometalate (2107 cm^{-1}).[7,15] This shift is consistent with other PBAs and is due to the loss of electron density from the 5σ orbital and the lack of backbonding via the N.[16] This suggests that the cyanide ligand is still C-bound to V^{III} and is consistent with the first prepared cyanovanadate(III)-containing PB-type material, $(NEt_4)_{0.02}Cr^{III}[V^{III}(CN)_6]_{0.98^-}(BF_4)_{0.08} \cdot 0.10MeCN$, where the 2136 cm^{-1} absorption was assigned to $V^{III}-CN-Cr^{III}$ linkages.[8] Thus, **1** is formulated as $Mn_{1.5}[V^{III}(CN)_6] \cdot 0.30MeCN$.[17]

Compound **2** has a ν_{CN} absorption at 2081 cm^{-1} (hwhh: 50 cm^{-1}), which is decreased from the 2107 cm^{-1} absorption observed in $[V^{III}(CN)_6]^{3-}$.[18] This 2081 cm^{-1} absorption is, however, more consistent with $Fe^{II}-C\equiv N-V^{III}$ linkages rather than $Fe^{II}-N\equiv C-V^{III}$ linkages being present. Formation of this motif requires linkage isomerization to occur, and several examples of PB-structured materials exhibiting linkage isomerization have been reported.[19] In addition, $(NEt_4)_4[Fe^{II}(CN)_6]$ exhibits ν_{CN} absorptions at 2030(s), 2050(vs), and 2080(m),[20] and upon bridging to another metal ion, a shift to higher energy is expected. PB itself, which has $Fe^{II}-C\equiv N-Fe^{III}$ linkages, exhibits a broad ν_{CN} absorption at 2080 cm^{-1} (hwhh: 47 cm^{-1}).[21] Therefore, **2** is formulated as $Fe^{II}_{0.5}V^{III}[Fe^{II}(CN)_6] \cdot 0.85MeCN$, which results from the occurrence of linkage isomerization.

Compound **3** exhibits two ν_{CN} absorptions at 2121 and 2161 cm^{-1} (hwhh: 30 and 25 cm^{-1}, respectively). Both absorptions are at higher energy with respect to the 2107 cm^{-1} absorption observed for $[V^{III}(CN)_6]^{3-}$, consistent with **1** having $Co^{II}-N\equiv C-V^{III}$ linkages. However, because of the presence of two ν_{CN} absorptions, other alternative binding motifs can be considered. For example, if linkage isomerization occurs, then formation of a $Co^{II}-C\equiv N-V^{III}$ linkage will occur. PB-type materials that have this type of binding, where the cyanide is C-bound to the Co^{II} ion, are limited because cyanocobalt(II) complexes are not hexacoordinate but are tetra- or pentacoordinate,[22] e.g. $[Co^{II}(CN)_5]^{3-}$.[23] $(NEt_4)_3[Co^{II}(CN)_5]$ has an observed ν_{CN} absorption at 2080

(13) Exposure to air results in oxidation, leading to the growth of a vanadyl absorption at ∼980 cm^{-1}. Samples were confirmed to have the absence of this peak before analyses were performed.

(14) Miller, J. S.; Kravitz, S. H.; Kirschner, S.; Ostrowski, P.; Nigrey, P. J. *J. Chem. Educ.* **1978**, *55*, 181.

(15) Compound **1** also exhibits a small shoulder at 2090 cm^{-1} (Figure S1 in the Supporting Information), which is likely due to a small amount of either (a) linkage isomerization that results in the formation of $Mn^{II}-CN-V^{III}$ linkages or (b) electron transfer that forms $Mn^{III}-NC-V^{III}$ linkages. Distinguishing between these two possible linkages is not trivial because of the low intensity of the shoulder, and only the main absorption at 2130 cm^{-1} was discussed.

(16) Nakamoto, K. In *Infrared and Raman Spectra of Inorganic and Coordination Compounds Part B: Applications in Coordination, Organometallic, and Bioinorganic Chemistry*, 5th ed.; Wiley-Interscience: New York, 1997; p 111.

(17) Linkage isomerization of the cyanide ligand to form $Mn^{II}-CN-V^{III}$ linkages was considered; however, it was previously shown that a $[Mn^{II}(CN)_6]^{4-}$-containing PBA, $K_2Mn^{II}[Mn^{II}(CN)_6]$, has a 2055-cm^{-1} ν_{CN} absorption. Entley, W. R.; Girolami, G. S *Inorg. Chem.* **1994**, *33*, 5165.

(18) A weak shoulder at 2120 cm^{-1} was also observed for **2** (Figure S1 in the Supporting Information), and it is attributed to a small amount of $Fe^{II}-NC-V^{III}$ linkages arising from incomplete linkage isomerization.

(19) (a) Brown, D. B.; Shriver, D. F.; Anderson, S. E. *Inorg. Chem.* **1965**, *4*, 725. (b) Buschmann, W. E.; Ensling, J.; Gütlich, P.; Miller, J. S. *Chem.—Eur. J.* **1999**, *5*, 3019.

(20) Eller, S.; Dieter Fischer, R. *Inorg. Chem.* **1990**, *29*, 1289.

(21) Ghosh, S. N. *J. Inorg. Nucl. Chem.* **1974**, *36*, 2465.

(22) Carter, S. J.; Foxman, B. M.; Stulh, L. S. *Inorg. Chem.* **1986**, *25*, 2888.

cm^{-1},[24] and Beauvais and Long reported the first PBA, i.e., Co^{II}$_3$[Co^{II}(CN)$_5$]$_2$.[25] This compound, which orders magnetically at 38 K, has a strong ν_{CN} absorption at 2178 cm^{-1}. This value is in good agreement with the 2161 cm^{-1} absorption, suggesting that Co^{II}−C≡N−V^{III} linkages may be present.

An alternative formulation involves electron transfer, along with linkage isomerization, occurring between Co^{II} and V^{III} sites and resulting in the formation of Co^{III}−C≡N−V^{II} linkages. K$_3$[Co^{III}(CN)$_6$] has a reported ν_{CN} absorption at 2129 cm^{-1},[26] and several PB-structured materials containing this anion with a Co^{III}−C≡N−M binding motif have been reported with ν_{CN} absorptions ranging from 2165 to 2180 cm^{-1}.[27] The observed 2161 cm^{-1} absorption also suggests that Co^{III}−C≡N−V^{II} linkages are possible. Distinguishing between the Co^{II}−C≡N−V^{III} or Co^{III}−C≡N−V^{II} linkages cannot be directly obtained from the ν_{CN} absorptions alone; however, when considering the order of lability for cyanometalates, [M^{III}(CN)$_6$]$^{3−}$ (V > Mn >> Cr > Fe ∼ Co), it is more likely the latter linkage has been formed because of the stability of the [Co^{III}(CN)$_6$]$^{3−}$ anion.[28] Hence, **3** has both Co^{II}−N≡C−V^{III} and Co^{III}−C≡N−V^{II} linkages present in the structure, which can be assigned to the 2121 and 2161 cm^{-1} absorptions, respectively. It is determined that the ratio of these two linkages cannot be directly obtained from the IR spectra; therefore, further insight is needed from the magnetic analyses to draw any further conclusions on the chemical formulation of this compound (vide infra). For now, we can represent this compound with the generic formula (NEt$_4$)$_{0.10}$Co^{II}$_{1.5−a}$V^{II}$_a$[Co^{III}(CN)$_6$]$_a$[V^{III}(CN)$_6$]$_{1−a}$(BF$_4$)$_{0.10}$·0.35-MeCN (a < 1).

Compound **4** exhibits a strong ν_{CN} absorption at 2168 cm^{-1} (hwhh: 28 cm^{-1}). Again, this absorption is shifted to higher energy with respect to [V^{III}(CN)$_6$]$^{3−}$, and it is an average of ∼43 cm^{-1} higher than the observed ν_{CN} absorption in compounds **1** and **3**, which were assigned to M^{II}−N≡C−V^{III} linkages. Because of this large shift for the Ni^{II} compound, isomerization of the desired Ni^{II}−N≡C−V^{III} linkages are considered. Linkage isomerization in **4** would result in the formation of Ni^{II}−C≡N−V^{III}. Cyanonickelate(II) complexes can exist as tetracyanonickelates, and in some cases pentacyanonickelates. In the solid state, [Ni^{II}(CN)$_4$]$^{2−}$ has been reported to have a ν_{CN} absorption occurring at 2142 cm^{-1},[29] whereas [Ni^{II}(CN)$_5$]$^{3−}$ has four observed ν_{CN} bands at 2076,

2100, 2114, and 2127 cm^{-1}.[30] It was also reported that Ni^{II}(CN)$_2$·1.5H$_2$O,[31] an extended network solid, was shown to have the presence of Ni^{II}−C≡N−Ni^{II} linkages,[8,32] and the ν_{CN} absorption for this binding motif was reported to be 2170 cm^{-1}.[33] In addition, numerous other extended network materials containing the four-coordinate [Ni^{II}(CN)$_4$]$^{2−}$ with its cyanides bridging to another metal have an observable range of ν_{CN} absorptions from 2143 to 2195 cm^{-1}.[34] Hence, the 2168 cm^{-1} ν_{CN} absorption is more consistent with the cyanides being C-bound to Ni^{II} than the V^{III} forming Ni^{II}−C≡N−V^{III} linkages. Therefore, **3** undergoes linkage isomerization, forming (NEt$_4$)$_{0.20}$V^{III}[Ni^{II}(CN)$_4$]$_{1.6}$·0.10MeCN. This formulation is further confirmed by magnetic analysis (vide infra).

Compounds **1**–**4** also have small amounts of both coordinated (ν_{CN} = 2286 ± 3 and 2313 ± 2 cm^{-1}) and noncoordinated MeCN (ν_{CN} = 2252 cm^{-1}). Upon exposure to air, these absorptions rapidly disappear and a simultaneous growth of ν_{OH} absorptions are observed. Thus, MeCN can be easily displaced by water upon exposure to moisture, and it is likely that MeCN in these materials is on the surface and/or in the interstitial lattice sites, as previously reported.[35] The IR spectra for these compounds also show trace amounts of the NEt$_4$$^+$ cation as well as anion (SbF$_6$$^−$ in **1** or BF$_4$$^−$ in **2**–**4**) that were minimized, but not eliminated, by thoroughly washing the solids with MeCN. The samples chosen for analyses were verified to have minimal amounts of these ions by IR analyses.

Thermal Stability. The thermal properties of compounds **1**–**4** were analyzed by TGA/MS (Figures S2−S5 in the Supporting Information). In general, each compound showed loss of MeCN and cyanide at 50 °C, followed by a continuous gradual mass loss up to 600 °C, all resulting in black residues. Because of this gradual mass loss, attributed to simultaneous solvent loss and decomposition, the temperatures at which these events occur are indistinguishable. Nevertheless, the total mass losses were determined to be 26.0, 56.7, 49.7, and 46.5%. Overall, these materials are not very thermally stable because of their facile loss of MeCN and cyanide at relatively low temperatures (∼50 °C); therefore, all materials were stored at −25 °C, and exposure

(23) (a) Alexander, J. J.; Gray, H. B. *J. Am. Chem. Soc.* **1967**, *89*, 3356. (b) Griffith, W. P.; Lane, J. R. *J. Chem. Soc., Dalton Trans.* **1972**, *158*. (c) White, D. A.; Solodar, A. J.; Baizer, M. M. *Inorg. Chem.* **1972**, *11*, 2160. (d) Brown, L. D.; Raymond, K. N. *Inorg. Chem.* **1975**, *14*, 2590.
(24) White, D. A.; Solodar, A. J.; Baizer, M. M. *Inorg. Chem.* **1972**, *11*, 2160.
(25) Beauvais, L. G.; Long, J. R. *J. Am. Chem. Soc.* **2002**, *124*, 12096.
(26) Jones, L. H. *Inorg. Chem.* **1963**, *2*, 777.
(27) (a) Ludi, A.; Güdel, H. U. *Helv. Chim. Acta* **1968**, *51*, 2006. (b) Shiver, D. F.; Brown, D. B. *Inorg. Chem.* **1969**, *8*, 42. (c) Griebler, W.-D.; Babel, D. *Z. Naturforsch.* **1982**, *37b*, 832. (d) Buchold, D. H. M.; Feldmann, C. *Chem. Mater.* **2007**, *19*, 2276.
(28) (a) Taube, H. *Chem. Rev.* **1952**, *50*, 69. (b) Basolo, F.; Pearson, R. G. *Mechanism of Inorganic Reactions: A Study of Metal Complexes in Solution*, 2nd ed.; John Wiley and Sons Inc.: New York, 1967; p 157. (c) Atwood, J. D. *Inorganic and Organometallic Reaction Mechanisms*, 2nd ed.; Wiley-VCH:New York, 1997; p 84.
(29) Kubas, G. J.; Jones, L. H. *Inorg. Chem.* **1974**, *13*, 2816.
(30) Raymond, K. N.; Corfield, P. W. R.; Ibers, J. A. *Inorg. Chem.* **1968**, *7*, 1362.
(31) Ludi, A.; Hügi, R. *Helv. Chim. Acta* **1967**, *50*, 1283.
(32) The Ni^{II}−C≡N−Ni^{II} linkages come from square-planar [Ni^{II}(CN)$_4$]$^{2−}$ sites bridging through the cyanide to octahedral [Ni^{II}(NC)$_4$(OH$_2$)$_2$]$^{2−}$ sites.
(33) (a) El-Sayed, M. F. A.; Sheline, R. K. *J. Inorg. Nucl. Chem.* **1958**, *6*, 187. (b) Ludi, A.; Hügi, R. *Helv. Chim. Acta* **1968**, *51*, 349.
(34) (a) Özbay, A.; Yurdakul, Ş. *J. Mol. Struct.* **1995**, *349*, 13. (b) Karacan, N.; Kantarcý, Z.; Akyüz, S. *Spectrochim. Acta, Part A* **1996**, *52*, 771. (c) Yurdakul, Ş; Güllüoğlu, M. T.; Küçükgüldal, D.; Taþdelen, M. *J. Mol. Struct.* **1997**, *408–409*, 319. (d) Yurdakul, Ş; Bahat, M. *J. Mol. Struct.* **1997**, *412*, 97. (e) Kasap, E.; Özbay, A.; Özçelik, S. *Spectrosc. Lett.* **1997**, *30*, 491. (f) Akyüz, S. *J. Mol. Struct.* **1998**, *449*, 23. (g) Yurdakul, Ş.; Yilmaz, C. *Vib. Spectrosc.* **1999**, *21*, 127. (h) Serbakan, T. R.; Sağlam, S.; Kasap, E.; Kantarci, Z. *Vib. Spectrosc.* **2000**, *24*, 249. (i) Bahat, M.; Yurdakul, Ş. *Spectrochim. Acta, Part A* **2002**, *58*, 933. (j) Akyuz, S. *J. Mol. Struct.* **2003**, *651–653*, 541. (k) Chen, X.-Y.; Shi, W.; Xia, J.; Cheng, P.; Zhao, B.; Song, H.-B.; Wang, H.-G.; Yan, S.-P.; Liao, D.-Z.; Jiang, Z.-H. *Inorg. Chem.* **2005**, *44*, 4263. (l) Yeung, W.-F.; Kwong, H.-K.; Lau, T.-C.; Gao, S.; Szeto, L.; Wong, W.-T. *Polyhedron* **2006**, *25*, 1256.
(35) Buschmann, W. E.; Miller, J. S. *Inorg. Chem.* **2000**, *39*, 2411.

Table 2. Summary of Magnetic Properties for **1**–**4**

	1	**2**	**3**	**4**
χT_{obs}, emu·K/mol[a]	5.29	2.20	2.35	0.95
χT_{calc}, emu·K/mol[b]	7.39	2.66	3.14[c]	0.83
$\chi T(T-\theta)_{calc}$, emu·K/mol	5.54	2.61	2.99[c]	0.82
θ, K (Curie–Weiss)	−4	−6	−15	−3
θ, K (Néel)	−100			
T_N, K (dc)	90			
T_{onset}, K (ZFC)	35			
T_b, K (ZFC/FC)	10			
T_c, K (ac)	12			
T_f, K (ac)	11.5			
φ (ac)	0.029			
H_{cr}, Oe	65			
M, emu·Oe/mol, (at 90 kOe)	21 000	8000	10 800	7180
M_{rem}, emu·Oe/mol	780			

[a] At room temperature. [b] Calculated spin-only values. [c] These χT values are for $a = 1$ in $(NEt_4)_{0.10}Co^{II}_{1.5-a}V^{II}_a[Co^{III}(CN)_6]_a[V^{III}(CN)_6]_{1-a}(BF_4)_{0.10}\cdot 0.35MeCN$.

to ambient temperatures was minimized. Drying of the samples before analyses was performed at room temperature to avoid any thermal decomposition at elevated temperatures.

PXRD. Generally, PBAs adopt a fcc structure with a unit cell lattice constant (*a*) ranging from 9.9 to 10.9 Å;[4,5] however, the diffraction patterns of **1**–**4** showed weak broad peaks indicative of being completely amorphous, and none of the patterns could be indexed to a fcc structure. Because of their amorphous nature, these materials are structurally disordered, and this results in small sample-to-sample variations in both the structural and magnetic properties. The synthesis of more crystalline samples was attempted by varying the addition rate in the synthesis; however, all samples were concluded to be amorphous regardless of the synthetic procedure.

Magnetic Susceptibility. The temperature dependencies of the susceptibility, $\chi(T)$, of **1**–**4** were measured at 500 Oe between 5 and 300 K. From these data, it was concluded that only compound **1** exhibits bulk magnetic ordering. The magnetic properties of **1**–**4** are summarized in Table 2 and are individually discussed below.

Compound 1. 1 has a room temperature χT value of 5.29 emu·K/mol that is substantially lower than the spin-only value of 7.39 emu·K/mol for $S = 1$ and $g = 1.82$ (V^{III})[7] and $S = \frac{5}{2}$ and $g = 2.00$ (Mn^{II}).[36] Above 250 K, $\chi(T)$ was fit to the Curie–Weiss expression $\chi \propto (T - \theta)^{-1}$, with $\theta = -4$ K, suggesting that antiferromagnetic coupling dominates the short-range exchange.[37] As the temperature is lowered, $\chi T(T)$ gradually increases until ~100 K, increasing more rapidly to a maximum of 163 emu·K/mol at 28 K and then finally decreasing rapidly down to 43.3 emu·K/mol at 5 K (Figure 1). The rise in $\chi T(T)$ to a maximum is consistent with the onset of magnetic ordering at ~70 K from an extrapolation of the steepest slope in $\chi T(T)$ to zero. The exact ordering temperature, T_c, is determined via alternate methods. Ferrimagnetic ordering is anticipated because of the negative θ value determined from the Curie–Weiss fit. Also consistent with ferrimagnetic ordering is the expected minimum in

(36) Watanabe, T. *J. Phys. Soc. Jpn.* **1961**, *16*, 1131.
(37) Caution should be taken with the Curie−Weiss fit of compound **1** because of the small temperature range that was used to fit the $\chi^{-1}(T)$ data (250−300 K).

Figure 1. $\chi T(T)$ (●) and $\chi^{-1}(T)$ (○) for **1**. The fit to Néel's hyperbolic equation (eq 1) is displayed with a solid line. The sample was cooled in a zero applied field to 5 K, and data were measured upon warming in a 500 Oe applied field.

$\chi T(T)$ above T_c. This results from short-range antiferromagnetic correlations and causes a cancelation of spins as the temperature is lowered.[38,39] This expected minimum, however, is not observed for **1**. The absence of this minimum may be explained by a lack of thermal energy at room temperature needed to completely compensate for magnetic coupling energy, which causes thermal randomization of the electron spins, and the $\chi T(T)$ data will likely have a minimum occurring at elevated temperatures. Hence, the reported θ value is an effective θ and not the true value.

For materials exhibiting an onset of ferrimagnetic ordering, the θ value can also be determined from Néel's theory[39] (eq 1), where C and θ are the Curie and Weiss constants, respectively, and θ' and ζ are proportional to $\eta_A\eta_B C(\eta_A - \eta_B)$ and $\eta_A\eta_B C$ (where η_i is the fractional occupancy of each sublattice site), respectively. Above 110 K, $\chi^{-1}(T)$ for **1** was fit to eq 1 with a Néel temperature, T_N, of 90 K and a θ value of −100 K. Using this θ value, $\chi T(T - \theta)_{calc}$ was calculated to be 5.54 emu·K/mol, which is more consistent with the observed room temperature χT value of 5.29 emu·K/mol. The less than ideal hyperbolic shape of the fit to the $\chi^{-1}(T)$ data suggests the presence of several spin domains. Inside these domains, the spins are well ordered just above 90 K; however, these domains do not correlate throughout the bulk material until a lower temperature is obtained.

$$\chi^{-1} = \frac{T - \theta}{C} - \frac{\zeta}{T - \theta'} \qquad (1)$$

Low-field $M(T)$ measurements are used to determine key information about an ordering system, and low-field $M_{ZFC}(T)/M_{FC}(T)$ (ZFC and FC represent zero-field-cooled and field-cooled, respectively) of **1** shows the onset of magnetic ordering, T_{onset}, below 35 K (by extrapolation of the steepest slope to T where $M = 0$) and a blocking temperature, T_b, of 10 K (Figure 2). T_b is the temperature where the $M_{ZFC}(T)$ and $M_{FC}(T)$ magnetizations converge, and below this, the

(38) (a) Stumpf, H. O.; Pei, Y.; Kahn, O.; Sletten, J.; Renard, J. P. *J. Am. Chem. Soc.* **1993**, *115*, 6738. (b) Stumpf, H. O.; Ouahab, L.; Pei, Y.; Bergerat, P.; Kahn, O. *J. Am. Chem. Soc.* **1994**, *116*, 3866.
(39) (a) Néel, L. *Ann. Phys.* **1948**, *3*, 137. (b) Smart, J. S. *Am. J. Phys.* **1955**, *23*, 356.
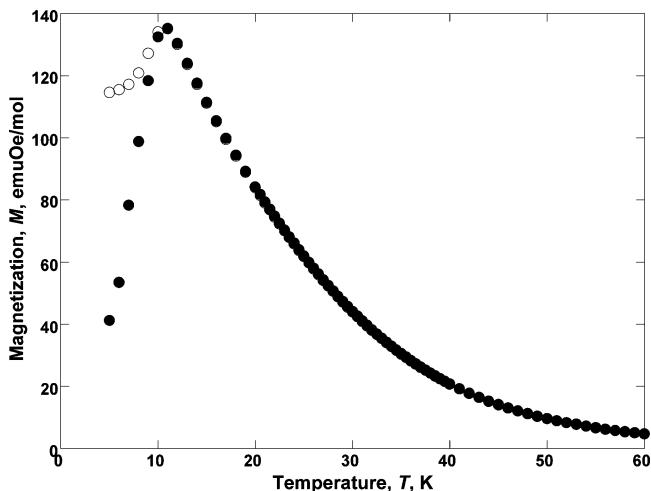
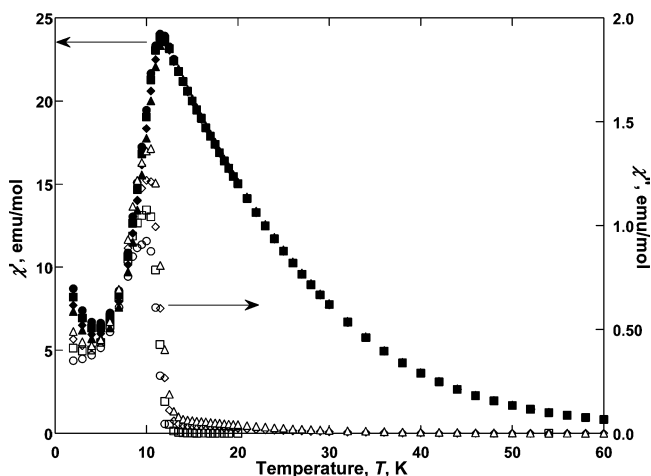**Figure 2.** 5 Oe M_{ZFC} (●) and M_{FC} (○) data for **1**.

Figure 3. Observed $\chi'(T)$ (closed symbols) and $\chi''(T)$ (open symbols) ac responses for **1** at 33 (○), 100 (□), 333 (◇), and 1000 (△) Hz in zero applied field.

Figure 4. Magnetic hysteresis curve for **1**.

temperature is irreversibile (or hysteresis) in these magnetizations as a result of entering the magnetically ordered state. The decrease in magnetization below the peak in the $M_{ZFC}(T)$/$M_{FC}(T)$ data is consistent with this sample having strong antiferromagnetic interactions, resulting in ferrimagnetic behavior.

The frequency-dependent in-phase, $\chi'(T)$, and out-of-phase, $\chi''(T)$, components of the alternating current (ac) susceptibility can also be used to determine the magnetic ordering temperatures. In a zero applied direct current (dc) field, **1** exhibits a response in both $\chi'(T)$ and $\chi''(T)$ with a magnetic ordering temperature of 12 K from the initial rise in the $\chi''(T)$ data upon cooling (Figure 3). This ordering temperature is consistent with the blocking temperature obtained in the $M_{ZFC}(T)$ and $M_{FC}(T)$ data. **1** has an observable frequency dependence, $\varphi = 0.029$, which is attributed to a spin- or cluster-glass behavior.[40] Spin- or cluster-glass behavior has been reported for other PBAs and is indicative of a more disordered and/or amorphous material.[7,35,41] This is consistent with the PXRD data, where **1** was shown to be amorphous and structurally disordered (vide supra). The temperature at which the maximum in the $\chi'(T)$ data becomes frequency-dependent corresponds to the temperature at which the
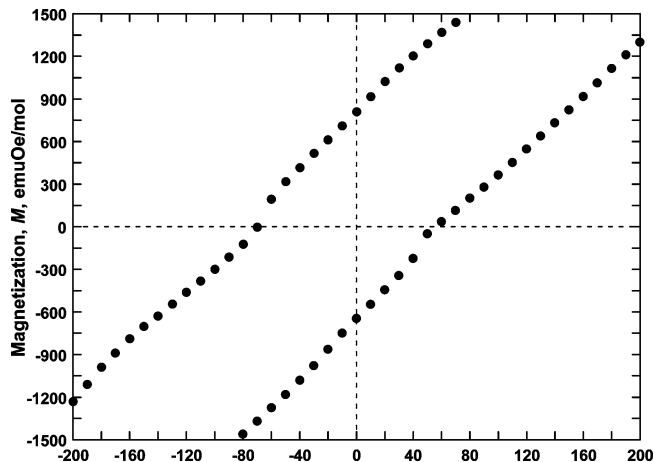
magnetic moments of this disordered material become frozen, and this is termed the freezing temperature, T_f. T_f for **1** was determined [by a peak in the $\chi'(T)$ at 33 Hz] to be 11.5 K. The spin- or cluster-glass behavior supports the hypothesis that there are small ferrimagnetic domains separated by a sea of paramagnetic spins (vide supra). At T_f, the spins in these ferrimagnetic domains are randomly frozen and result in an overall net moment, causing an increase in $\chi(T)$ and a response in $\chi_{ac}(T)$.

$M(H)$ measurements at 2 K show that **1** does not saturate even at 90 kOe, where a magnetization value of 21 000 emu·Oe/mol is observed (Figure S6 in the Supporting Information). At low temperature, the spins in this system (for V^{III}, $S = 1$ and $g = 1.82$,[7] and for Mn^{II}, $S = 5/2$ and $g = 2.00$[36]) should be antiferromagnetically aligned, resulting in an expected saturation magnetization value of 31 700 emu·Oe/mol. Hysteresis was also observed for **1** at 2 K (coercive field, H_{cr}, of 65 Oe) with a remanent magnetization, M_{rem}, of 730 emu·Oe/mol (Figure 4).

1 is one of the first reported PBA with $[V^{III}(CN)_6]^{3−}$ incorporated into the structure, leading to M−N≡C−V^{III} linkages. This material is best described as ferrimagnet, exhibiting a cluster-glass behavior. At 90 K, ferromagnetic spin domains grow in size, resulting in a superparamagnetic-like effect with an overall increase in the $\chi T(T)$ data. When compound **1** is submerged in liquid N_2 and removed, the sample becomes attracted to a magnet (displayed in the Table of Contents picture), which is in accordance with the presence of a superparamagnetic-like state above the observed critical temperature of 12 K. As the temperature is decreased further, these spin domains grow until bulk magnetic ordering is obtained at 12 K. At this temperature,

(40) Mydosh, J. A. In *Spin Glasses: An Experimental Introduction*; Taylor and Francis: London, 1993; p 67. φ is a parameter indicative of the amount of spin disorder in a material known as spin-glass behavior: $\varphi = \Delta T_{max}/[T_{max}(\Delta \log \omega)]$, where ΔT_{max} = difference between the peak maxima of the temperatures at the high and low frequencies, T_{max} = peak maximum of the temperature at low frequency, and $\Delta \log \omega$ = difference in the logarithms of the high and low frequencies (ω).

(41) (a) Buschmann, W. E.; Ensling, J.; Gütlich, P.; Miller, J. S. *Chem.—Eur. J.* **1999**, *5*, 3019. (b) Sendek, M.; Csach, K.; Kavecansky, V.; Lukácová, M.; Marysko, M.; Mitróová, Z.; Zentko, A. *Phys. Status Solidi A* **2003**, *196*, 225.
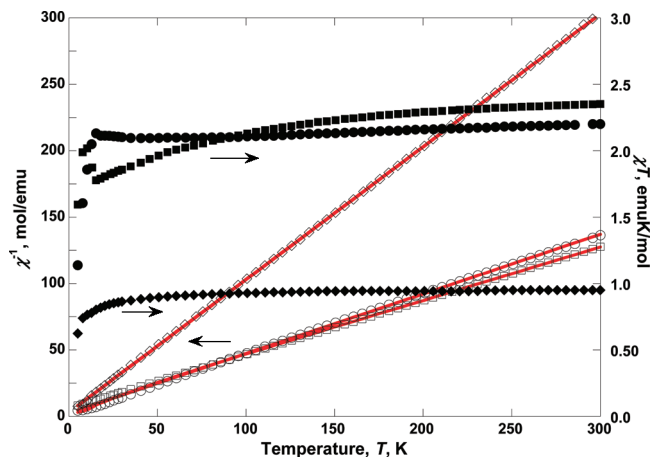
Figure 5. $\chi T(T)$ (closed symbols) and $\chi^{-1}(T)$ (open symbols) for **2** (circles), **3** (squares), and **4** (diamonds). Fits to the Curie–Weiss law, $\chi \propto (T - \theta)^{-1}$, are displayed with solid lines. Samples were cooled in a zero applied field to 5 K, and data were measured upon warming in a 500 Oe applied field.

the spin domains become frozen ($T_f = 11.5$ K), resulting in the observed χ_{ac} response.

Compound 2. 2 has a room temperature χT value of 2.20 emu·K/mol that is only slightly lower than the spin-only value of 2.66 emu·K/mol for V^{III}, $S = 1$ and $g = 1.82$,[7] and for Fe^{II}, $S = 2$ and $g = 2.21$ (Figure 5).[42a] If linkage isomerization does not occur, then **2** would be formulated as $Fe^{II}_{1.5}[V^{III}(CN)_6] \cdot 0.85MeCN$ and all Fe^{II} ions would be in a high-spin environment. This would lead to a spin-only χT value at room temperature of 6.32 emu·K/mol for V^{III}, $S = 1$ and $g = 1.82$,[7] and for Fe^{II}, $S = 2$ and $g = 2.21$.[42a] This spin-only $\chi T(T)$ value drastically exceeds the observed value of 2.20 emu·K/mol, indicative that linkage isomerization has occurred and **2**'s correct formulation is $Fe^{II}_{0.5}V^{III}[Fe^{II}(CN)_6] \cdot 0.85MeCN$. Above 50 K, $\chi(T')$ could be fit to the Curie–Weiss expression $\chi \propto (T - \theta)^{-1}$ with $\theta = -6$ K, suggesting that antiferromagnetic coupling dominates the short-range exchange. This is in accordance with reported literature ranges (-8 to $+23$ K) for other hexacyanoferrate(II) PBAs.[43] The shape of the $\chi T(T)$ data is consistent with **2** being paramagnetic, with no long-range order being observed. Using the θ value of -6 K, $\chi T(T - \theta)_{calc}$ was calculated to be 2.61 emu·K/mol, which is consistent with the observed room temperature χT value, confirming **2**'s formulation of $Fe^{II}_{0.5}V^{III}[Fe^{II}(CN)_6] \cdot 0.85MeCN$.

The 2 K $M(H)$ data display that **2** does not saturate at 50 kOe, where a magnetization of 8000 emu·Oe/mol is observed (Figure S6 in the Supporting Information). The shape of the $M(H)$ curve and the inability to saturate are indicative of a paramagnetic material. In summary, **2** is a paramagnetic material with weak antiferromagnetic coupling ($\theta = -6$ K).

The absence of bulk magnetic ordering is likely caused by the presence of the diamagnetic $[Fe^{II}(CN)_6]^{4-}$ ($S = 0$) bridging the paramagnetic ions (V^{III} and Fe^{II}), resulting in the distance between paramagnetic sites being greater than 10 Å. This large distance causes no correlation of the spins throughout the bulk materials.

Compound 3. 3 has a room temperature χT value of 2.35 emu·K/mol. From the discussion of the IR data above, **3** undergoes a partial linkage isomerization, resulting in the presence of two types of bridging cyanides [$Co^{II}-N{\equiv}C-V^{III}$ (2121 cm^{-1}) and $Co^{III}-C{\equiv}N-V^{II}$ (2161 cm^{-1})]. However, the ratio of these linkages cannot be obtained directly from the intensities of the IR absorptions. In an attempt to elucidate the ratio of these linkages, the calculated χT values of the two limiting compositions are investigated ($a = 0$ and $a = 1$). If $a = 0$, then the formulation of **3** is $(NEt_4)_{0.10}Co^{II}_{1.5}[V^{III}(CN)_6](BF_4)_{0.10} \cdot 0.35MeCN$. With this formulation, a spin-only value of 5.58 emu·K/mol (for V^{III}, $S = 1$ and $g = 1.82$,[7] and for Co^{II}, $S = 3/2$ and $g = 2.60$[42b]) is calculated. This calculated χT value is much higher than the observed room temperature value of 2.35 emu·K/mol; thus, this formulation is unlikely. If $a = 1$, then the formulation of **3** is $(NEt_4)_{0.10}Co^{II}_{0.5}V^{II}[Co^{III}(CN)_6]$-$(BF_4)_{0.10} \cdot 0.35MeCN$. This formulation results in a spin-only value of 3.14 emu·K/mol (for V^{II}, $S = 3/2$ and $g = 1.82$;[7] for Co^{II}, $S = 3/2$ and $g = 2.60$;[42b] and for diamagnetic $[Co^{III}(CN)_6]^{3-}$, $S = 0$), which is more consistent with the observed room temperature value of 2.35 emu·K/mol. Above 50 K, χ (T) could be fit to the Curie–Weiss expression $\chi \propto (T - \theta)^{-1}$ with $\theta = -15$ K, suggesting that antiferromagnetic coupling dominates the short-range exchange (Figure 5), and this θ value is consistent with the literature values of -31 K reported for $Co^{II}_3[Co^{III}(CN)_5]_2$.[25] Using this θ value (-15 K), $\chi T(T - \theta)_{calc}$ was determined to be 5.31 and 2.99 emu·K/mol for $a = 0$ and 1, respectively. In the latter case ($a = 1$), no $Co^{II}-N{\equiv}C-V^{III}$ linkages remain that would result in the no observable ν_{CN} absorption assigned to these linkages (2121 cm^{-1}). This is not the case for **3**, where the 2121 cm^{-1} absorption is slightly more intense than the 2161 cm^{-1} absorption (the observed ratio of the $Co^{III}-C{\equiv}N-V^{II}$: $Co^{II}-N{\equiv}C-V^{III}$ linkages is 0.93). If the ν_{CN} absorptions for these two stretching modes had equivalent intensities, the complete composition could be obtained directly from this ratio. The actual composition of **3** is still somewhat of a mystery; however, from the room temperature χT value, it is clear that the formulation exists somewhere between these two stoichiometric limits and is closer to the latter formulation of $(NEt_4)_{0.10}Co^{II}_{0.5}V^{II}[Co^{III}(CN)_6](BF_4)_{0.10} \cdot 0.35MeCN$ than the former one. Because the exact formulation could not be obtained from these studies, a generic composition of $(NEt_4)_{0.10}Co^{II}_{(1.5-a)}V^{II}_a[Co^{III}(CN)_6]_a[V^{III}(CN)_6]_{1-a}(BF_4)_{0.10} \cdot 0.35MeCN$ will be used to describe this material.[44]

The 2 K $M(H)$ data show that **3** does not saturate at 90 kOe, where a magnetization value of 10 800 emu·Oe/mol is observed (Figure S6 in the Supporting Information). The

(42) (a) Boudreaux, E. A.; Mulay, L. N. *Theory and Applications of Molecular Paramagnetism*; Wiley-Interscience: New York, 1976; p 203. (b) Boudreaux, E. A.; Mulay, L. N. *Theory and Applications of Molecular Paramagnetism*; Wiley-Interscience: New York, 1976; p 214.

(43) (a) Egan, L.; Kamenev, K.; Papanikolaou, D.; Takabayashi, Y.; Margadonna, S. *J. Am. Chem. Soc.* **2006**, *128*, 6034. (b) Martínez-Garcia, R.; Knobel, M.; Reguera, E. *J. Phys. Chem. B* **2006**, *110*, 7296.

(44) Another method of determining the oxidation states of the Co and V metal ions in **3** is via X-ray photoelectron spectroscopy; however, at this time, we do not have the capability to perform these measurements.

shape of the $M(H)$ curve and the inability to saturate are indicative of a paramagnetic material. Hence, **3** is a paramagnet with moderate antiferromagnetic coupling ($\theta = -15$ K). The chemical formulation is unclear, but a generic formulation of $(NEt_4)_{0.10}Co^{II}_{1.5-a}V^{II}_a[Co^{III}(CN)_6]_a[V^{III}-(CN)_6]_{1-a}(BF_4)_{0.10} \cdot 0.35MeCN$ ($a < 1$) can be used to represent the binding motifs in this new material. The absence of bulk magnetic ordering is likely caused by the inherent structural disorder, presence of diamagnetic $[Co^{III}(CN)_6]^{3-}$, and number of different paramagnetic species in **3**.

Compound 4. 4 has a room temperature χT value of 0.95 emu·K/mol that is only slightly larger than the spin-only value of 0.83 emu·K/mol for $S = 1$ and $g = 1.82^7$ for V^{III} and $S = 0$ for Ni^{II}. The room temperature χT value confirms the presence of diamagnetic square-planar $[Ni^{II}(CN)_4]^{2-}$, which was formed upon linkage isomerization of the cyanide ligand. Above 5 K, $\chi(T)$ could be fit to the Curie–Weiss expression (Figure 5) with $\theta = -3$ K and $g = 1.96$, suggesting that antiferromagnetic coupling dominates the short-range exchange. Using this θ value, $\chi T(T - \theta)_{calc}$ was determined to be 0.82 emu·K/mol. In $Ni^{II}(CN)_2 \cdot 1.5H_2O^{31}$ and $[Cu^{II}(HL)]_2[Ni^{II}(CN)_4]$ (where $H_2L = $ 3,9-dimethyl-4,8-diazaundeca-4,8-diene-2,10-dione dioxime),^{45} similar magnetic data are reported, where both compounds contain diamagnetic $[Ni^{II}(CN)_4]^{2-}$ ($S = 0$) and a second paramagnetic metal ion, octahedral Ni^{II} ($S = 1$) in the former and square-planar Cu^{II} ($S = \frac{1}{2}$) in the latter. The magnetic data for both compounds are representative of the paramagnetic metal sites in these bimetallic systems.

The 2 K $M(H)$ data show that **4** does not saturate at 90 kOe, where a magnetization value of 7180 emu·Oe/mol is observed (Figure S6 in the Supporting Information). The shape of the $M(H)$ curve and the inability to saturate are indicative of a paramagnetic material. Thus, **4** is a paramag-

(45) Ray, A.; Dutta, D.; Mondal, P. C.; Sheldrick, W. S.; Mayer-Figge, H.; Ali, M. *Polyhedron* **2007**, *26*, 1012.

netic material with weak antiferromagnetic coupling ($\theta = -3$ K), and its formulation as $(NEt_4)_{0.20}V^{III}[Ni^{II}(CN)_4]_{1.6} \cdot 0.10MeCN$ fits well for a paramagnetic V^{III} ($S = 1$) with $g = 1.96$. The absence of bulk magnetic ordering is a result of diamagnetic $[Ni^{II}(CN)_4]^{2-}$ sites creating a larger separation between paramagnetic sites.

Conclusion

Incorporation of $[V^{III}(CN)_6]^{3-}$ into PB-structured materials has proven to be synthetically challenging. The reaction of $[V^{III}(CN)_6]^{3-}$ with $[M^{II}(NCMe)_6]^{2+}$ [M = Cr,^{7} Mn (**1**), Fe (**2**), Co (**3**), and Ni (**4**)] in a MeCN solution results in new PB-type materials; however, only one compound in this series maintains the $[V^{III}(CN)_6]^{3-}$ complex after the synthesis is performed (M = Mn). All of the other compounds in this series have either electron transfer (M = Cr, Co) and/or partial (M = Co) or complete (M = Fe, Ni) linkage isomerization of the cyanide ligand, resulting in the formation of M–C≡N–V linkages. The three compounds exhibiting linkage isomerization (M = Fe, Co, Ni) are paramagnetic down to low temperatures with only moderate ($\theta = -15$ K for Co) to weak ($\theta = -3$ K for Ni) short-range antiferromagnetic interactions. When M = Mn, a ferrimagnetic cluster-glass material is formed that magnetically orders at 12 K (via ac measurements). At 2 K, this compound has an observable coercivity of 65 Oe and remanent magnetization of 730 emu·Oe/mol.

Supporting Information Available: Figures S1–S6 are available free of charge via the Internet at http://pubs.acs.org.

IC701845P